Materials Research. 2015; 18(1): 85-91
DOI: http://dx.doi.org/10.1590/1516-1439.272614

Microwave Assisted Synthesis and Sintering of $Ba_{0.5}Sr_{0.5}Co_{0.8}Fe_{0.2}O_{3-\delta}$ Perovskite

***Rafael Bianchini Nuernberg*[a]*, Márcio Raymundo Morelli*[a]**

[a]*Department of Materials Engineering, Federal University of São Carlos – UFSCar, São Carlos, SP, Brazil*

Received: October 2, 2014; Revised: July 1, 2015

$Ba_{0.5}Sr_{0.5}Co_{0.8}Fe_{0.2}O_{3-\delta}$ (BSCF) perovskite-type oxide is currently one of the most promising materials for applications in solid-oxide fuel cells (SOFCs), protonic ceramic fuel cells (PCFCs), oxygen separation membranes, and catalytic membranes for methane conversion. BSCF powder synthesis has received considerable attention and new synthesis methods have been proposed to obtain nanoscale powders with high chemical homogeneity. In this study, BSCF perovskite powder has been successfully prepared by microwave assisted combustion in aqueous solution. The synthesized powder was characterized by DSC, BET, XRD, and SEM. BSCF powder presented phase homogeneity, high specific surface area (9.93 g/m^2) and nanometric crystallite size (23nm). The microwave sintering has been conducted in different conditions of dwell time and temperature. The influence of the temperature and the dwell time on microstructure was evaluated by optical microscopy. The results showed that microwave sintering could achieve the same densification compared to conventional sintering with only 10% of processing time. This shorter processing time has resulted in a reduction of grain size of up to 46.5%, compared to conventional sintering.

Keywords: *MIEC, BSCF, microwave assisted combustion synthesis, microwave sintering*

1. Introduction

$Ba_{0.5}Sr_{0.5}Co_{0.8}Fe_{0.2}O_{3-\delta}$ (BSCF) is a mixed ionic-electronic conducting (MIEC) oxide which has received attention as a promising material in advanced technologies, such as, solid-oxide fuel cells (SOFCs) or protonic ceramic fuel cells (PCFCs) cathodes, and membrane reactors in air separation and catalytic conversion of methane[1,2]. The BSCF compound was originally developed to application in oxygen permeable ceramic membranes. In this application, an oxygen partial pressure gradient between the membrane sides acts as the driving force for the oxygen transport across the membrane. The oxygen permeation process through these membranes involves oxygen exchange on the membrane surfaces and migration of oxygen anions through the crystal lattice via oxygen vacancies until to reach the opposite side and the exchange reverse process occurs[1-5]. In particular, the BSCF perovskite is known by its high oxygen diffusivity and extremely low surface resistance to oxygen reduction, and incorporation into crystal lattice[1,2,6-8].

While the search for novel materials with improved transport and mechanical properties have been continued, research efforts were also directed towards optimization of the membrane architecture. An architecture composed of a dense layer permeable only to oxygen and a porous layer of high specific surface area is usually employed to increase the oxygen permeability. In order to maximize the oxygen permeation flux, the membrane thickness is often reduced. However, with decreasing membrane thickness, the mechanical strength is affected. Furthermore, the membrane becomes surface limiting and the flux no longer increase in proportion as decreasing membrane thickness. The most employed strategy is to use thick porous layer with high permeability and high specific surface area, in order to improve the mechanical properties and increase the available area to exchange reactions. Thereby, this architecture development suggests the using of starting powders with nanometer particles size and high specific surface area[4,8-11].

Consequently, BSCF powders synthesis has become a subject of great relevance and the BSCF perovskite has been synthesized by several methods: conventionally by solid state reaction[12,13], combustion synthesis reaction[14,15], co-precipitation method[8,16], complexing method[5,11,12], and others[17]. Moreover, the use of microwave heating together with these synthesis methods has emerged as a novel route to produce materials in nanoscale[17]. On the other hand, the sintering process is important for membrane consolidation and microstructural development. The control of this stage is indispensable to retain a thinner microstructure in dense layer aiming to improve the mechanical properties of these membranes. Regarding the porous layer, the control of grain size aiming to avoid grain growth, results an increase of membrane specific surface[5,8,16,18-20]. The use of microwave energy in ceramic materials sintering has been widely studied over the last decades. Some of the most important advantages of microwave heating are volumetric energy absorption and enhancement of the mass transport. Therefore, higher heating rates and shorter processing time can be employed in microwave heating. Thus, the final microstructure can be better controlled, resulting in materials with thinner microstructure and better functional properties in comparison to conventional heating methods[21-25]. Accordingly, the aims of this present study are microwave synthesis and sintering of BSCF perovskite in

*e-mail: Nuernbergrafael@gmail.com

order to evaluate the effectiveness of this heating method to control particles size of BSCF powder, and densification and microstructural development of BSCF phase.

2. Experimental

All the reagents used in the experiments were acquired from Synth Analytical Reagents and were used without further purification. BSCF powder was synthesized by microwave assisted combustion synthesis. Stoichiometric amounts of metal nitrates corresponding to BSCF phase ($Ba(NO_3)_2$, $Sr(NO_3)_2$, $Co(NO_3)_2.6H_2O$, $Fe(NO_3)_3.9H_2O$) and the fuel urea ($(CO(NH_2)_2)$) were dissolved in deionized water into a silica crucible at temperature of 80 °C. After that, the crucible was placed in a domestic microwave oven (2.45 GHz, 900W) for 8 min. Firstly, the solution boils, undergoes dehydration, and increases the concentration of regents in solution followed by decomposition with the evolution of large amount of gases. Next, the solution reaches the spontaneous combustion temperature, burns, instantly vaporizes, and becomes a dark powder with friable appearance. The as-prepared powder was analyzed by X-ray diffraction (XRD) using a SIEMENS D-5005 diffractometer with CuKa radiation ($\lambda = 0.15418$ nm) and by differential scanning calorimetry / thermogravimetry (DCS / TG) using a equipment Netzsch Sta 449c under heating rate of 10 °C/min. In order to crystallize BSCF phase, the powder was treated at temperature of 900 °C according to data from DCS/TG analysis and, the treatment time was kept in two hours according to some reports[14,15]. Then, BSCF powder was subject to wet ball milling in ethanol for 12 h in order to decrease agglomeration and to provide easier densification in sintering stage. The structure and crystallinity of BSCF powder were again characterized by XRD. The powder morphology was examined by scanning electron microscope (SEM) using an equipment FEI Inspect s50. Specific surface area was indirectly measured using ASAP 2020 through adsorption-desorption nitrogen isotherms and estimated by BET method. Dilatometric analysis of a compacted sample was performed in a contact dilatometer Netzsch 402C under heating rate of 5 °C/min from 25 °C to 1050 °C.

As for the sintering stage, the synthetized BSCF powder was pressed in disk-shape samples using a 10mm diameter stainless die under uniaxial pressure of 250MPa for 3 min. The sintering stage was conducted in several dwell times and temperatures, using conventional and microwave heating. Table 1 shows the different conditions of dwell time and temperature used in this study. It was used heating rates of 5 °C/min and 50 °C/min in conventional and microwave sintering, respectively. The microwave equipment and its installation scheme were reported in previous study[23], and the heating power was kept in 2.1KW. Bulk density of the sintered discs was measured by water immersion technique based on Archimedes' principle after two hours immersed in boiling water. Relative density was determined using the theoretical density of BSCF phase. The dense ceramic disks were polished and thermally attached 25 °C below the sintering temperature without dwell time and under heating rate of 15 °C/min. The microstructure of samples was evaluated by optical microscopy and the distribution and average grain size were estimated by using Image J software considering projected area diameter of the measured grain area.

3. Results and Discussion

3.1. Synthesis

XRD patterns of as-prepared powder and heat-treated BSCF powder are presented in Figure 1. In as-prepared XRD patterns, several basal reflections can be seen which makes the phases identifications difficult; surely corresponding to the main phase and other secondary phases. On the other hand, XRD pattern of heat-treated BSCF powder has presented complete formation of cubic perovskite BSCF. The main reflection planes of BSCF phase are indicated in Figure 1 according to some reports[15,16]. The average crystallite size was evaluated from XRD broadening peak using the Scherrer's equation[26] which was found to be ~23 nm. The specific surface area of BSCF powder and the corresponding size estimated by BET diameter equation[27] were found to be 9.93 m^2/g and 107.8 nm, respectively.

Morphology and characteristics of BSCF powder can be seen in SEM micrographs, which is shown in Figure 2. The micrograph under magnification of 10000 X shown in Figure 2a presents a more general view of the synthesized powder, which presents a homogeneous morphology. Figure 2b shows a micrograph under magnification of 60000 X, where the particles of BSCF powder can be seen better, presenting a size smaller than 1 μm. Dilatometric analysis of a green disk-shape BSCF was made in order to observe the temperature of maximum densification rate of synthesized powder. Figure 3 shows the shrinkage curve and the first derivative curve. It can be seen by means of the

Table 1. Conditions of dwell time and temperature for conventional and microwave sintering.

Conventional Sintering			Microwave Sintering		
Sample	**Temperature (°C)**	**Time(min)**	**Sample**	**Temperature (°C)**	**Time(min)**
C975-300	975	300	M975-30	975	30
C1000-300	1000	300	M1000-30	1000	30
C1025-300	1025	300	M1025-30	1025	30
C1050-300	1050	300	M1050-30	1050	30
C1025-60	1025	60	M1025-6	1025	6
C1025-120	1025	120	M1025-12	1025	12
C1025-600	1025	600	M1025-60	1025	60

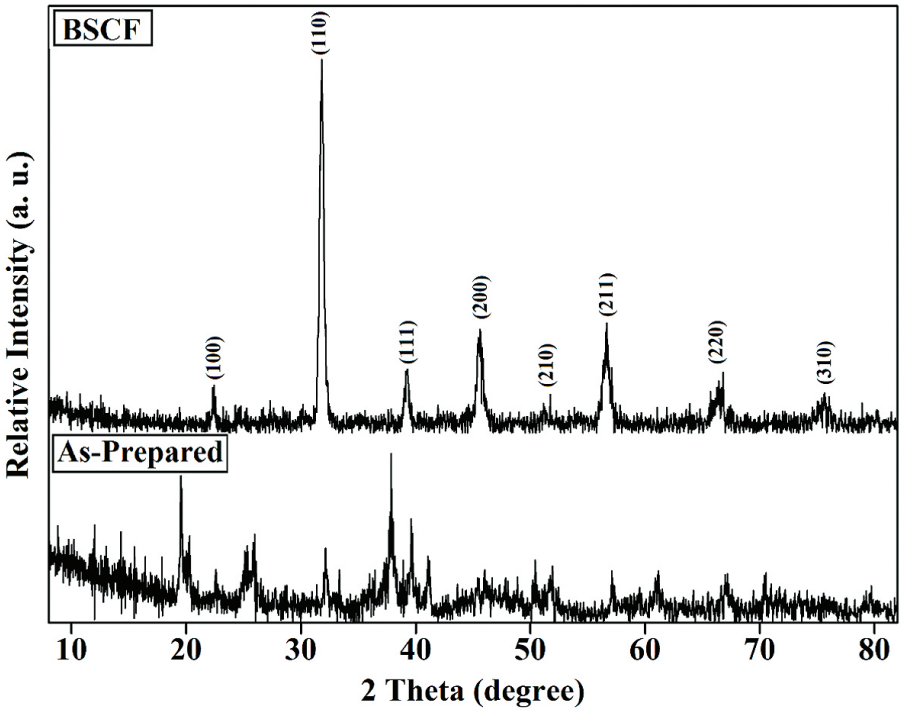

Figure 1. XRD patterns of as-prepared powder and BSCF powder after heat treatment at 900°C.

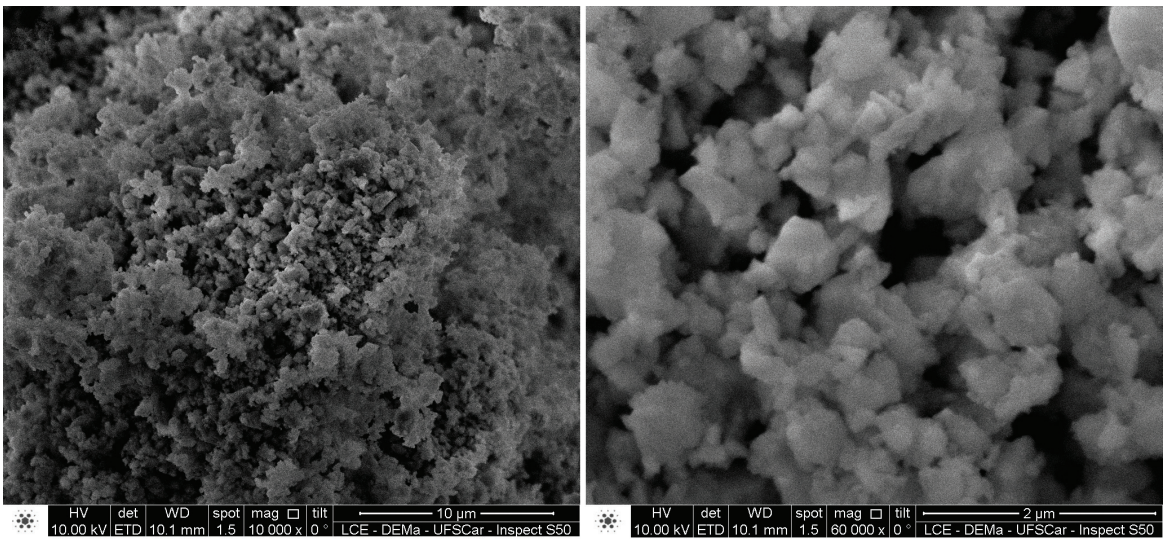

(a) (b)

Figure 2. SEM micrographs of BSCF powder in two different magnifications: 10000X (a) and 60000X (b).

first derivative curve that the maximum densification rate occurs around 975 °C. From this result were determined the sintering conditions to both sintering methods.

3.2. Sintering

The synthetized BSCF powder has presented excellent sinterability reaching relative densities superior to 97%. Figure 4 shows the dependence of the relative density and the average grain size on the temperature and the dwell time, for the two sintering methods. By means of comparison between Figure 4a (conventional sintering) and Figure 4b (microwave sintering), it can be noticed that the dependence of both average grain size and relative density on temperature follows a trend which seems to be independent of the sintering method. Nevertheless, although the relative densities in two heating methods were found in the same range, the average grain size reached in microwave sintering was about 44% smaller than conventional sintering. In case the variable is the dwell time, in short times sintering, there is a significant difference between relative densities

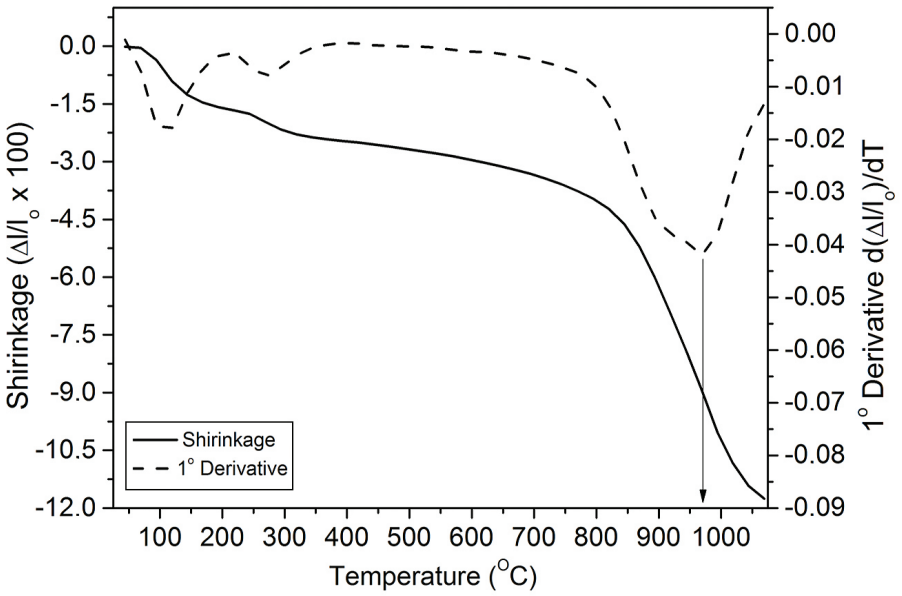

Figure 3. Dilatometric analysis of a green disk-shape of BSCF synthesized powder.

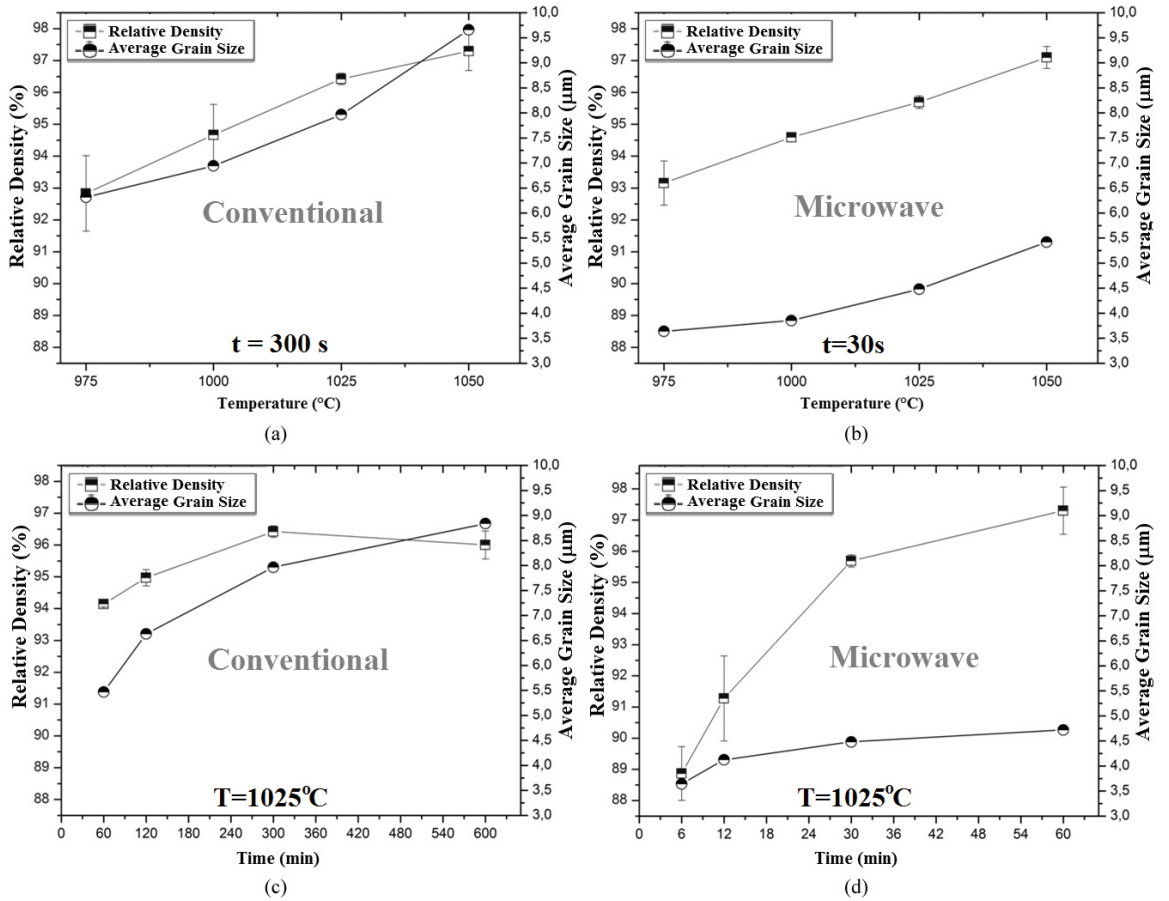

Figure 4. Dependence of relative density and average grain size with: i) temperature in (a) conventional heating and (b) microwave heating; ii) dwell time in conventional heating (c) and microwave heating (d).

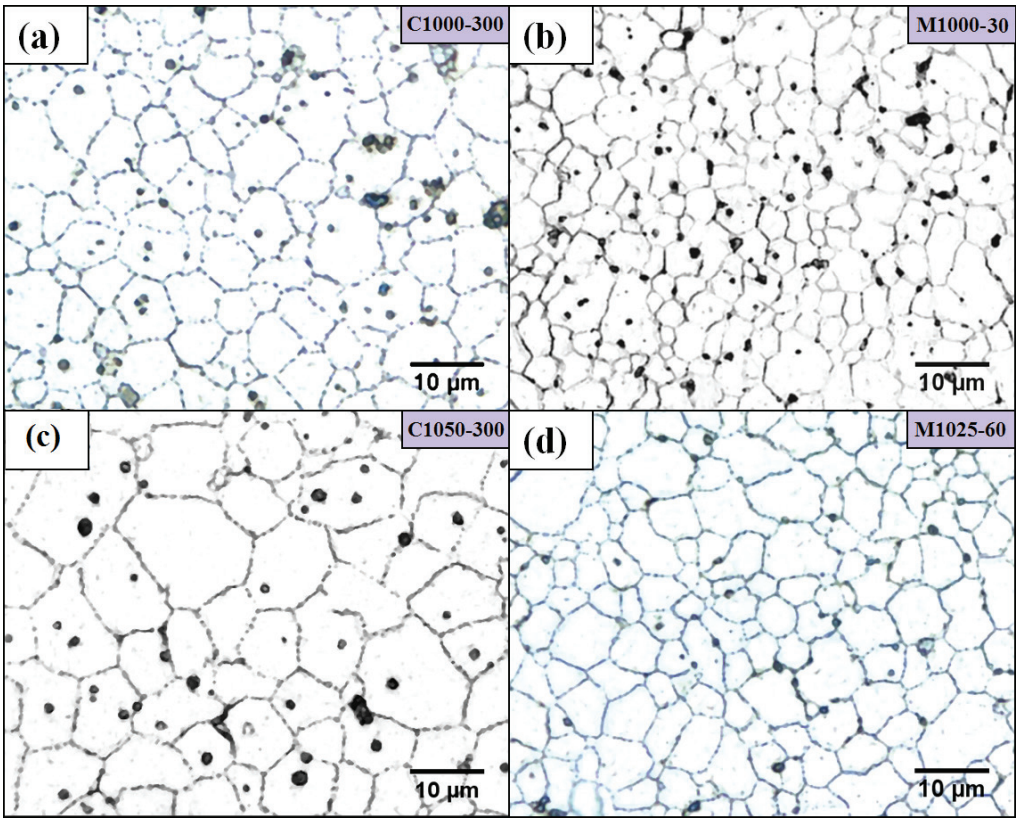

Figure 5. Optical micrographs under 1000X magnification for the samples C1000-300 (a), M1000-30 (b), C1050-300 (c) and M1025-60 (d).

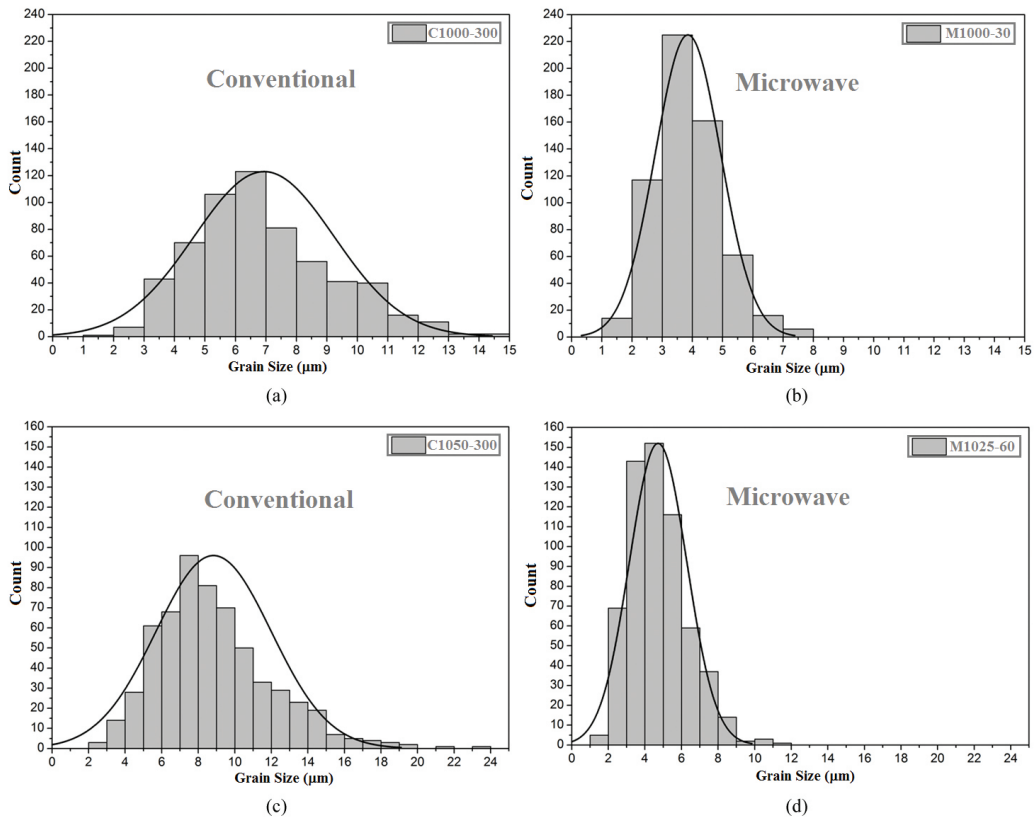

Figure 6. Grain size distribution for the samples C1000-300 (a), M1000-30 (b), C1050-300 (c) and M1025-60 (d).

in conventional (Figure 4c) and microwave sintering (Figure 4d). Under dwell time of 60 minutes in conventional heating and 6 minutes in microwave heating, the relative densities reached were 94.1 ± 0.1% and 88.9 ± 0.9%, respectively. However, this difference between heating methods is overcome in long times sintering. Concerning to microstructure, the microwave sintering retains grain size of up to 46.5% smaller than convectional sintering.

Figure 5 shows four optical micrographs under magnification of 1000X corresponding to samples C1000-300 (a), M1000-30 (b), C1050-300 (c), and M1025-60 (d). Samples C1000-300 and M1000-30 have presented the same relative densities within the error tolerances; 94.7 ± 0.9% and 94.6 ± 0.1%, respectively. Comparing the micrograph of samples C1000-300 and M1000-30 , despite the same density, the effectiveness of microwave sintering on control of final microstructure of BSCF phase can be readily observed. The same effect occurs in samples C1050-300 and M1025-60, which presented relative density of 97.3% ± 0.6% and 97.3± 0.8%, respectively. In all these cases, microwave sintering resulted in a more refined microstructure than conventional sintering. This grain size reducing in microwave sintering can be attributed to shorter dwell time (10 times shorter) and higher heating rate (10 times higher), comparatively to conventional heating. Another advantage noted in microwave sintering is the effect in the grain size distribution. Figure 6 shows grain size distribution for each one of the microstructure presented in Figure 5. The use of microwave sintering resulted in a grain size distribution narrower than conventional sintering. This effect was observed in shorter dwell times and lower temperatures sintering (Figure 6a and Figure 6b) as well as in longer dwell times and higher temperature sintering (Figure 6c and Figure 6d). It is well known that the more homogeneous microstructures usually lead to better functional properties.

4. Conclusion

The BSCF perovskite was successfully synthesized using microwave-assisted combustion method followed by heat treatment. The synthesized powder shows a set of interesting characteristics to membrane development such as, phase homogeneity, high specific surface area, nanometric crystallite size, and submicrometric particle size. High densities can be reached even at temperature as low as 975°C. Microwave sintering has proven effectiveness in densification of BSCF perovskite. In the most of sintering conditions used, microwave sintering reaches the same densification of conventional sintering with only 10% of processing time. The processing time reduction has resulted in more homogeneous and finer microstructure related to size and grain size distribution. These results suggest the use of microwave synthesis and sintering in processing of oxygen separation and catalytic membranes as well as fuel cells cathodes in order to develop architecture with better oxygen permeation properties, improving the efficiency of these technologies.

Acknowledgements

The authors are grateful to the CNPq and the PPG-CEM/UFSCar for their financial support, and to the laboratory of synthesis and processing of ceramic materials (LASP) for their support given in the experimental part of this work.

References

1. Zhou W, Ran R and Shao Z. Progress in understanding and development of Ba0.5Sr0.5Co0.8Fe0.2O3-δ based cathodes for intermediate-temperature solid-oxide fuel cells: A review. *Journal of Power Sources*. 2009; 192(2):231-246. http://dx.doi.org/10.1016/j.jpowsour.2009.02.069.
2. Sunarso J, Baumann S, Serra JM, Meulenberg WA, Liu S, Lin YS, et al. Mixed ionic-electronic conducting (MIEC) ceramic-based membranes for oxygen separation. *Journal of Membrane Science*. 2008; 320(1-2):13-41. http://dx.doi.org/10.1016/j.memsci.2008.03.074.
3. Zeng P, Chen Z, Zhou W, Gu H, Shao Z and Liu S. Re-evaluation of Ba0.5Sr0.5Co0.8Fe0.2O3-δ perovskite as oxygen semi-permeable membrane. *Journal of Membrane Science*. 2007; 291(1-2):148-156. http://dx.doi.org/10.1016/j.memsci.2007.01.003.
4. Jiang Q, Nordheden KJ and Stagg-Williams SM. Oxygen permeation study and improvement of Ba0.5Sr0.5Co0.8Fe0.2Ox perovskite ceramic membranes. *Journal of Membrane Science*. 2011; 369(1-2):174-181. http://dx.doi.org/10.1016/j.memsci.2010.11.073.
5. Baumann S, Schulze-Küppers F, Roitsch S, Betz M, Zwick M, Pfaff EM, et al. Influence of sintering conditions on microstructure and oxygen permeation of Ba0.5Sr0.5Co0.8Fe0.2O3-δ (BSCF) oxygen transport membranes. *Journal of Membrane Science*. 2010; 359(1-2):102-109. http://dx.doi.org/10.1016/j.memsci.2010.02.002.
6. Baumann FS, Fleig J, Habermeier HU and Maier J. Ba0.5Sr0.5Co0.8Fe0.2O3-δ thin film microelectrodes investigated by impedance spectroscopy. *Solid State Ionics*. 2006; 177(35-36):3187-3191. http://dx.doi.org/10.1016/j.ssi.2006.07.057.
7. Baumann FS, Maier J and Fleig J. The polarization resistance of mixed conducting SOFC cathodes: A comparative study using thin film model electrodes. *Solid State Ionics*. 2008; 179(21-26):1198-1204. http://dx.doi.org/10.1016/j.ssi.2008.02.059.
8. Ahmadrezaei M, Muchtar A, Muhamad N, Tan CY and Majlan EH. Electrochemical and microstructural characteristics of nanoperovskite oxides Ba0.5Sr0.5Co0.8Fe0.2O3-δ (BSCF) for solid oxide fuel cells. *Ceramics International*. 2013; 39(1):439-444. http://dx.doi.org/10.1016/j.ceramint.2012.06.045.
9. Niehoff P, Baumann S, Schulze-Küppers F, Bradley RS, Shapiro I, Meulenberg WA, et al. Oxygen transport through supported Ba0.5Sr0.5Co0.8Fe0.2O3-δ membranes. *Separation and Purification Technology*. 2014; 121:60-67. http://dx.doi.org/10.1016/j.seppur.2013.07.002.
10. Kovalevsky AV, Kharton VV, Snijkers FMM, Cooymans JFC, Luyten JJ and Marques FMB. Oxygen transport and stability of asymmetric SrFe(Al)O3−δ - SrAl2O4 composite membranes. *Journal of Membrane Science*. 2007; 301(1-2):238-244. http://dx.doi.org/10.1016/j.memsci.2007.06.028.

11. Hong WK and Choi GM. Oxygen permeation of BSCF membrane with varying thickness and surface coating. *Journal of Membrane Science*. 2010; 346(2):353-360. http://dx.doi.org/10.1016/j.memsci.2009.09.056.
12. Tan L, Gu X, Yang L, Jin W, Zhang L and Xu N. Influence of powder synthesis methods on microstructure and oxygen permeation performance of Ba0.5Sr0.5Co0.8Fe0.2O3-δ perovskite-type membranes. *Journal of Membrane Science*. 2003; 212(1-2):157-165. http://dx.doi.org/10.1016/S0376-7388(02)00494-5.
13. Burriel M, Niedrig C, Menesklou W, Wagner SF, Santiso J and Ivers-Tiffée E. BSCF epitaxial thin films: Electrical transport and oxygen surface exchange. *Solid State Ionics*. 2010; 181(13-14):602-608. http://dx.doi.org/10.1016/j.ssi.2010.03.005.
14. Kovalevsky AV, Yaremchenko AA, Kolotygin VA, Shaula AL, Kharton VV, Snijkers FMM, et al. Processing and oxygen permeation studies of asymmetric multilayer Ba0.5Sr0.5Co0.8Fe0.2O3-δ membranes. *Journal of Membrane Science*. 2011; 380(1-2):68-80. http://dx.doi.org/10.1016/j.memsci.2011.06.034.
15. Liu B, Zhang Y and Zhang L. Characteristics of Ba0.5Sr0.5Co0.8Fe0.2O3-δ - La0.9Sr0.1Ga0.8Mg0.2O3−δ composite cathode for solid oxide fuel cell. *Journal of Power Sources*. 2008; 175(1):189-195. http://dx.doi.org/10.1016/j.jpowsour.2007.09.088.
16. Toprak MS, Darab M, Syvertsen G and Muhammed M. Synthesis of nanostructured BSCF by oxalate co-precipitation as potential cathode material for solid oxide fuels cells. *International Journal of Hydrogen Energy*. 2010; 35(17):9448-9454. http://dx.doi.org/10.1016/j.ijhydene.2010.03.121.
17. Shao Z, Zhou W and Zhu Z. Advanced synthesis of materials for intermediate-temperature solid oxide fuel cells. *Progress in Materials Science*. 2012; 57(4):804-874. http://dx.doi.org/10.1016/j.pmatsci.2011.08.002.
18. Wang H, Tablet C, Feldhoff A and Caro J. Investigation of phase structure, sintering, and permeability of perovskite-type Ba0.5Sr0.5Co0.8Fe0.2O3-δ membranes. *Journal of Membrane Science*. 2005; 262(1-2):20-26. http://dx.doi.org/10.1016/j.memsci.2005.03.046.
19. Salehi M, Clemens F, Pfaff EM, Diethelm S, Leach C, Graule T, et al. A case study of the effect of grain size on the oxygen permeation flux of BSCF disk-shaped membrane fabricated by thermoplastic processing. *Journal of Membrane Science*. 2011; 382(1-2):186-193. http://dx.doi.org/10.1016/j.memsci.2011.08.007.
20. Baumann S, Serra JM, Lobera MP, Escolástico S, Schulze-Küppers F and Meulenberg WA. Ultrahigh oxygen permeation flux through supported Ba0.5Sr0.5Co0.8Fe0.2O3-δ membranes. *Journal of Membrane Science*. 2011; 377(1-2):198-205. http://dx.doi.org/10.1016/j.memsci.2011.04.050.
21. Clark DE, Folz DC, Folgar CE and Mahmoud MM. What is microwave processing. In: Clark DE, Folz DC, Folgar CE and Mahmoud MM, editors. *Microwave solutions for ceramic engineer*. Ohio: John Wiley & Sons, 2005.
22. Charmond S, Carry CP and Bouvard D. Densification and microstructure evolution of Y-Tetragonal Zirconia Polycrystal powder during direct and hybrid microwave sintering in a single-mode cavity. *Journal of the European Ceramic Society*. 2010; 30(6):1211-1221. http://dx.doi.org/10.1016/j.jeurceramsoc.2009.11.014.
23. Menezes RR, Souto PM and Kiminami RHGA. Microwave hybrid fast sintering of porcelain bodies. *Journal of Materials Processing Technology*. 2007; 190(1-3):223-229. http://dx.doi.org/10.1016/j.jmatprotec.2007.02.041.
24. Oghbaei M and Mirzaee O. Microwave versus conventional sintering: a review of fundamentals, advantages and applications. *Journal of Alloys and Compounds*. 2010; 494(1-2):175-189. http://dx.doi.org/10.1016/j.jallcom.2010.01.068.
25. Bykov YV, Rybakov KI and Semenov VE. High-temperature microwave processing of materials. *Journal of Physics. D, Applied Physics*. 2001; 34(13):R55-R75. http://dx.doi.org/10.1088/0022-3727/34/13/201.
26. Mohebbi H, Ebadzadeh T and Hesari FA. Synthesis of nano-crystalline NiO-YSZ by microwave-assisted combustion synthesis. *Powder Technology*. 2009; 188(3):183-186. http://dx.doi.org/10.1016/j.powtec.2008.04.095.
27. Farhadi S, Momeni Z and Taherimehr M. Rapid synthesis of perovskite-type LaFeO3 nanoparticles by microwave-assisted decomposition of bimetallic La[Fe(CN)6]·5H2O compound. *Journal of Alloys and Compounds*. 2009; 471(1-2):L5-L8. http://dx.doi.org/10.1016/j.jallcom.2008.03.113.